Pharmacological Research 131 (2018) 150–163

Contents lists available at ScienceDirect

Pharmacological Research

journal homepage: www.elsevier.com/locate/yphrs

Dehydroevodiamine and hortiamine, alkaloids from the traditional Chinese herbal drug *Evodia rutaecarpa*, are I_{Kr} blockers with proarrhythmic effects *in vitro* and *in vivo*

Igor Baburin[a,*,1], Rosanne Varkevisser[b,1], Anja Schramm[c,1], Priyanka Saxena[a], Stanislav Beyl[a], Phillip Szkokan[a,d], Tobias Linder[a], Anna Stary-Weinzinger[a], Marcel A.G. van der Heyden[b], Marien Houtman[b], Hiroki Takanari[b], Malin Jonsson[b], Jet H.D. Beekman[b], Matthias Hamburger[c,1], Marc A. Vos[b,1], Steffen Hering[a,1]

[a] *Department of Pharmacology and Toxicology, University of Vienna, Althanstrasse 14, A-1090 Vienna, Austria*
[b] *Department of Medical Physiology, University Medical Center Utrecht, Yalelaan 50, 3584 CM Utrecht, The Netherlands*
[c] *Division of Pharmaceutical Biology, University of Basel, Klingelbergstrasse 50, 4056 Basel, Switzerland*
[d] *ChanPharm GmbH, Leidesdorfgasse 14, Top 6, 1190 Vienna, Austria*

ARTICLE INFO

Article history:
Received 24 August 2017
Received in revised form 9 February 2018
Accepted 20 February 2018
Available online 15 March 2018

Keywords:
Evodia
Dehydroevodiamine
Hortiamine
hERG
Action potential duration
Early afterdepolarization

ABSTRACT

Evodiae fructus is a widely used herbal drug in traditional Chinese medicine. *Evodia* extract was found to inhibit hERG channels. The aim of the current study was to identify hERG inhibitors in *Evodia* extract and to investigate their potential proarrhythmic effects. Dehydroevodiamine (DHE) and hortiamine were identified as I_{Kr} (rapid delayed rectifier current) inhibitors in *Evodia* extract by HPLC-microfractionation and subsequent patch clamp studies on human embryonic kidney cells. DHE and hortiamine inhibited I_{Kr} with IC_{50}s of 253.2 ± 26.3 nM and 144.8 ± 35.1 nM, respectively. In dog ventricular cardiomyocytes, DHE dose-dependently prolonged the action potential duration (APD). Early afterdepolarizations (EADs) were seen in 14, 67, 100, and 67% of cells after 0.01, 0.1, 1 and 10 μM DHE, respectively. The proarrhythmic potential of DHE was evaluated in 8 anesthetized rabbits and in 8 chronic atrioventricular block (cAVB) dogs. In rabbits, DHE increased the QT interval significantly by 12 ± 10% (0.05 mg/kg/5 min) and 60 ± 26% (0.5 mg/kg/5 min), and induced Torsade de Pointes arrhythmias (TdP, 0.5 mg/kg/5 min) in 2 rabbits. In cAVB dogs, 0.33 mg/kg/5 min DHE increased QT duration by 48 ± 10% ($P < 0.05^*$) and induced TdP in 2/4 dogs. A higher dose did not induce TdP. In human induced pluripotent stem cell-derived cardiomyocytes (hiPSC-CMs), methanolic extracts of Evodia, DHE and hortiamine dose-dependently prolonged APD. At 3 μM DHE and hortiamine induced EADs.

hERG inhibition at submicromolar concentrations, APD prolongation and EADs in hiPSC-CMs and dose-dependent proarrhythmic effects of DHE at micromolar plasma concentrations in cAVB dogs should increase awareness regarding proarrhythmic effects of widely used *Evodia* extracts.

1. Introduction

Herbal drugs are one of the cornerstones of traditional Chinese medicine (TCM). Wu Zhu Yu, the dried and nearly ripe fruit of *Evodia rutaecarpa*, is among the most popular and widely used herbal drugs in TCM. It is used as an analgesic, anti-emetic, for treatment of headache, gastrointestinal disorders, and menstrual complaints, or by means of external application against mouth ulcers [1]. However, in contrast to the elaborate preclinical safety evaluations [2,3]

Abbreviations: DHE, dehydroevodiamine; I_{Kr}, rapid delayed rectifier current; APD, action potential duration; EAD, early afterdepolarization; cAVB, chronic atrioventricular block; TdP, Torsade de Pointes arrhythmia; hiPSC-CM, human induced pluripotent stem cell-derived cardiomyocytes; TCM, traditional Chinese medicine; hERG, human Ether-a-go-go Related Gene; HEK, human embryonic kidney; MD, molecular dynamics; BVR, beat-to-beat variability of repolarization; STV, short-term variability; LV, left ventricle; RV, right ventricle; MAP, monophasic action potentials; EB, ectopic beats; VSD, voltage-sensitive dye; LED, light-emitting diode; PMT, photomultiplier; DMSO, dimethylsulfoxide; WT, wild type; SEB's, single ectopic beats; MEB's, multiple ectopic beats; FDA, Food and Drug Administration; CiPA, Comprehensive in vitro Proarrhythmia Assay.

* Corresponding author.
E-mail address: igor.baburin@univie.ac.at (I. Baburin).

[1] The authors contributed equally to this work.

https://doi.org/10.1016/j.phrs.2018.02.024

to which new drug molecules are subjected, herbal drugs are considered as safe on the basis of empirical knowledge from use over centuries. This may be an issue, in particular, with herbal drugs containing pharmacologically potent molecules, such as is the case for some TCM herbs. Use of some TCM herbal preparations have been associated with severe side effects, and even deaths due to organ failure, as was the case with a slimming product containing *Aristolochia fanchi*, an herbal drug with meanwhile well-understood nephrotoxic liabilities [4].

DHE is the major alkaloid of *Evodia rutaecarpa,* and is known to have cardiovascular effects. DHE causes bradycardia, hypotension, and vasorelaxation [5–7]. More detailed electrophysiological studies revealed interference with pacemaker activity and with several ion currents in the heart. In pacemaker cells from rabbit sinoatrial tissue, diastolic depolarization was inhibited, and the spontaneous cycle length increased [8]. Furthermore, DHE increased the APD in these cells, an effect that was also shown in rabbit papillary muscle, and in isolated guinea pig atrial and ventricular cardiomyocytes [8,9]. In isolated guinea pig cardiomyocytes, DHE (0.1 μM) inhibited outward potassium currents (delayed rectifier) by 50%, and higher concentrations resulted in additional blockage of inward calcium and sodium currents [9]. It is currently not known whether inhibition of hERG (human Ether-a-go-go Related Gene) contributes to DHE-induced prolongation of the cardiac APD.

hERG encodes the α-subunit of the rapid delayed rectifier K^+ channel which can be mainly found in human myocardium, where it plays a central role in the repolarization phase of the cardiac action potential [10–12]. Inhibition of repolarizing outward potassium currents (especially hERG channel inhibition) and APD prolongation are considered as risk factors for TdP, even though the relation between the factors is not very strong [13]. Therefore, investigation of possible effects on the surface ECG, and direct determination of proarrhythmic potential in suitable large animal models is recommended. We here identified DHE and hortiamine as potent hERG channel inhibitors in *Evodia* extracts. The effects of DHE (the major alkaloid in *Evodia*) on APD were evaluated in isolated cardiomyocytes from cAVB dogs. Anesthetized rabbits and cAVB dogs were used to evaluate whether the ion blocking actions of DHE indeed translate to QT prolongation and proarrhythmia *in vivo*. Additionally, proarrhythmic effects of Evodia extracts, DHE and hortiamine on APD were studied in hiPSC-CMs.

2. Methods

2.1. Electrophysiology and molecular modeling

2.1.1. Patch clamp studies on HEK 293 cells expressing hERG, $Na_V1.5$ and $Ca_V1.2$ channels

HEK (human embryonic kidney) 293 cells stably expressing hERG (a kind gift of Dr. January, University of Wisconsin-Madison, WI, USA) and $Na_V1.5$ channels (ChanPharm GmbH, Vienna, Austria) were cultured and harvested as previously described [14,15]. Currents through hERG and $Na_V1.5$ channels stably expressed in HEK 293 cells were studied within 8 h of harvest in the whole-cell configuration of the planar patch clamp technique (NPC-16 Patchliner®, Nanion Technologies GmbH, Munich, Germany) [16,17] making use of an EPC 10 patch clamp amplifier (HEKA, Lambrecht/Pfalz, Germany). Currents were low-pass filtered at 10 kHz using the internal Bessel filter of the EPC-10 and sampled at 25 kHz. The extracellular bath solution for hERG current recordings contained (in mM): NaCl 140, KCl 4, $CaCl_2$ 2, $MgCl_2$ 1, D-Glucose*H_2O 5 and HEPES 10 (pH 7.4 with NaOH). The intracellular solution for hERG current recordings contained (in mM): KCl 50, NaCl 10, KF 60, EGTA 20 and HEPES 10 (pH 7.2 with KOH). The extracellular bath solution for sodium current recordings contained (in mM): NaCl 20, KCl 4, $CaCl_2$ 1.8, $MgCl_2$ 0.75, choline chloride 120 and HEPES 5 (pH 7.4 with NaOH). The intracellular solution for sodium current recordings contained (in mM): CsF 120, CsCl 20, EGTA 5 and HEPES 5 (pH 7.4 with CsOH). NPC-16 Patchliner® was used for drug applications. The PatchMaster software v.2.65 (HEKA, Lambrecht/Pfalz, Germany) was used for data acquisition. The voltage protocol for hERG current recordings (see inset in Fig. 1C) was designed to simulate voltage changes during a cardiac action potential with a 300 ms depolarization to +20 mV (analogous to the plateau phase of the cardiac action potential), a repolarization for 300 ms to −50 mV (inducing a tail current) and a final step to the holding potential of −100 mV. The decreases in the resulting tail current amplitudes were taken as a measure of block development during a pulse train. Sodium currents were recorded in response to 10 ms pulses (0.2 Hz) from a holding potential of −120 mV to 0 mV, and the $Na_V1.5$ channel block was estimated as the decrease in the peak current amplitude during a pulse train.

For barium current measurements through $Ca_V1.2$ channels, HEK 293 cells were transfected and cultured as previously described [18]. Barium currents through $Ca_V1.2$ channels transiently expressed in HEK 293 cells were studied 36–48 h after transfection by manual patch clamp technique making use of an Axopatch 200A patch clamp amplifier (Molecular Devices, Inc., Sunnyvale, CA, USA). Currents were filtered at 5 kHz and sampled at 10 kHz. The extracellular bath solution for I_{Ba} recordings contained (in mM): $BaCl_2$ 20, $MgCl_2$ 1, choline chloride 90 and HEPES 10 (pH 7.4 with methanesulfonic acid). Patch pipettes with resistances of 1–4 MΩ were made from borosilicate glass (Harvard Apparatus, Cambridge, UK) and filled with intracellular solution that contained (in mM): CsCl 145, $MgCl_2$ 3, EGTA 10 and HEPES 10 (pH 7.25 with CsOH). Drugs were applied to cells under voltage clamp using a microminifold perfusion system. The pClamp software package v.10.0 (Molecular Devices, Inc., Sunnyvale, CA, USA) was used for data acquisition. Barium currents were recorded in response to 50 ms pulses (0.2 Hz) from a holding potential of −80 mV to +10 mV, and the $Ca_V1.2$ channel block was estimated as the decrease in the peak current amplitude during a pulse train.

2.1.2. Voltage clamp studies on Xenopus oocytes expressing hERG channels

For details see Supplemental Material.

2.1.3. Patch clamp and voltage clamp data analysis

Origin software v.7.0 (OriginLab Corp., Northampton, MA, USA) was employed for analysis and curve fitting. The cumulative concentration-inhibition curves were fitted using the Hill equation: $I_{hERG,drug}/I_{hERG,control} = (100 - A)/(1 + (C/IC_{50})^{nH}) + A$ in which IC_{50} is the concentration at which hERG inhibition is half-maximal, C is the applied drug concentration, A is the fraction of hERG current that is not blocked, and n_H is the Hill coefficient [19].

2.1.4. Docking and MD (molecular dynamics) simulations

Coordinates of the identified hERG blockers were generated with Gaussview 5 (Gaussian, Inc., Wallingford, CT, USA). The thoroughly validated homology model of the open hERG pore (model 6 of Stary et al. [20]) was used as starting point for docking analyses. Docking was performed with the program GOLD v5.2 (Cambridge Crystallographic Data Centre, Cambridge, U.K.) using the GOLD scoring function. The coordinates of the geometric center calculated among the Y652 and F656 residues were taken as binding site origin and both side chains were treated as flexible. The modeling software Pymol (Molecular Graphics System, Version 1.4.1; Schrodinger, LLC) was used to visualize and examine the interactions of DHE with the hERG cavity. The most frequent binding mode was used as a starting conformation for MD simulations. Simulations were performed with Gromacs v. 4.5.4 [21] as described

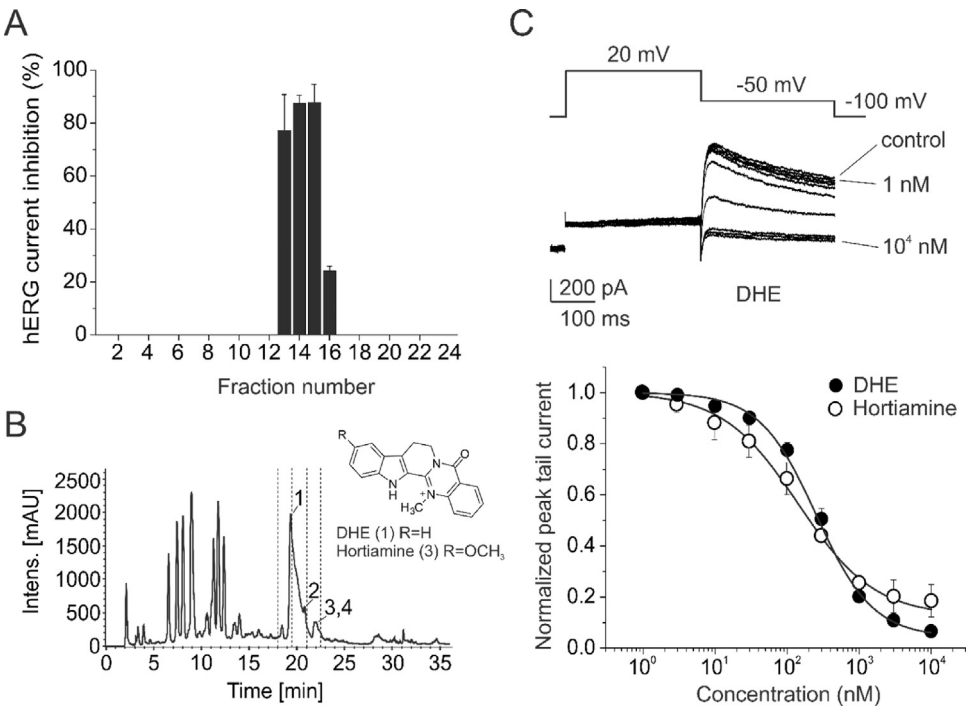

Fig. 1. Activity profiling of *Evodia rutaecarpa* methanolic extract and concentration-response relationship for block of hERG tail current by DHE and hortiamine in HEK 293 cells. (A, B) HPLC chromatogram (254 nm) of a semi-preparative separation of 5 mg extract and inhibition (in%) of hERG currents by 24 ninety-second fractions are shown. Compounds 1 and 3 were identified as DHE and hortiamine, respectively. (C) Upper part: Representative currents through hERG channels stably expressed in HEK 293 cells recorded in the absence (control) and presence of increasing concentrations of DHE (1 nM–10 μM) during 0.3 Hz pulse trains are shown. The voltage protocol is shown above. Lower part: DHE and hortiamine inhibited potassium current during repeated pulsing at 0.3 Hz at a holding potential of −100 mV in a concentration-dependent manner with the IC_{50} values of 253.2 ± 26.3 nM (n = 4) and 144.8 ± 35.1 nM (n = 4), respectively.

previously [22]. Briefly, the hERG model was embedded in an equilibrated 1-palmitoyl-2-oleoyl-sn-glycero-3-phosphocholine (POPC) membrane consisting of 242 lipid molecules by making use of the g_membed tool [23]. The amber99 sb force field [24] with lipid parameters taken from Berger et al. [25] and the TIP3P water model [26] were utilized. Geometry optimization and topology generation of the drugs was carried out with HF/6-31G*, implemented in Gaussian09 (Gaussian, Inc., Wallingford, CT, USA) [27] and antechamber [28] respectively. Prior to simulations, 1000 conjugate gradient energy-minimization steps were performed. Subsequently, the systems were equilibrated for 5 ns for each docked compound. During equilibration, the protein and the ligand were restrained with a force constant of 1000 kJ mol nm^{-2}, while the lipids, the ions, and the water were allowed to move freely. Each drug was simulated for 50 ns.

2.2. cAVB dog cardiomyocytes, anesthetized rabbits and cAVB dogs

Animal care and management were in adherence to the guidelines from Directive 2010/63/EU of the European Parliament. All animal experiments were approved by the Committee for Experiments on Animals of the Utrecht University, The Netherlands (approval reference numbers: 2012.11.02.039 (rabbits), 2013.11.08.088 (dogs)).

2.2.1. In vitro *action potential measurements in cAVB dog cardiomyocytes*

At the end of the final *in vivo* experiment and while still under anesthesia (see below), heparin (10 000 I.U., i.v.) was given and right side thoracotomy was performed after which the beating heart was excised from the thoracic cavity. Left ventricular cardiomyocytes were enzymatically isolated from chronically atrioventricular-blocked dog hearts (n = 5) as described previously [29]. Experiments were performed at 37 °C, a total of 17 cAVB cells were used. Action potentials were elicited with 2 ms current injections at a pacing rate of 0.5 Hz in whole current clamp mode, and recorded with PClamp9 software (Molecular devices, Sunnyvale, Ca, USA). Normal tyrode's solution (in mM): 140 NaCl, 5 KCl, 6 HEPES, 6 Glucose, 1.8 $CaCl_2$, 1 $MgCl_2$, pH 7.4 with NaOH and pipette solution (in mM): 110 KCl, 10 EGTA, 10 HEPES, 4 K_2-ATP, 5.17 $CaCl_2$, 1.42 $MgCl_2$, pH 7.2 with KOH were used. APD was measured at 90% repolarization. The cells were considered inducible (positive arrhythmogenic outcome) when at least three early afterdepolarizations (EADs) were observed. BVR (beat-to-beat variability of repolarization) was assessed using STV (short-term variability; based on 30 consecutive beats) which was calculated using the formula $STV = \Sigma|D_{n+1} - D_n|/[30\sqrt{2}]$ where D represents APD90 [30].

2.2.2. In vivo experiments – anesthetized rabbits

A total of 16 female New Zealand White rabbits (2.7–4.3 kg) were used. The animals were prepared and instrumented as described previously [29]. In short, anesthesia was induced with i.m. ketamine (35 mg/kg) and xylazine (5 mg/kg), and then maintained with inhaled isoflurane (1.5%) in O_2-supplemented air (1:1). After induction of anesthesia, the analgesic rimadyl (50 mg i.v.) was administered. After a 10 min stabilization period, 0.05 mg/kg DHE (n = 8) was infused over 5 min and the animals were observed for 25 min, hereafter this sequence was repeated using 0.5 mg/kg/5 min DHE. The second group of 7 rabbits were treated with two dosages of dofetilide (0.004 and 0.04 mg/kg/5 min) according to the same protocol. If necessary, an external defibrillator was used to terminate arrhythmias. After the experiments, while still under anesthesia (see below), heparin (10 000 I.U., i.v.) was given and mid-sternal thoracotomy was performed after which

the beating heart was excised from the thoracic cavity. One animal was excluded from the experiments due to technical issues.

2.2.3. In vivo *experiments – cAVB dogs*

Eight adult mongrel dogs (20–25 kg) were included in the study. The cAVB dog model was implemented as described earlier [31]. In short, the dogs were sedated with 10 mg methadone, 10 mg acepromazine and 0.5 mg atropine (i.m.). Hereafter, general anesthesia was induced by an intravenous bolus injection of 25 mg/kg sodium pentobarbital, anesthesia was maintained by inhaled isoflurane 1.5% in N_2O/O_2 (1:2). A screw-in transvenous pacemaker lead was advanced via the right jugular vein to the right ventricular apex and connected to an internal pacemaker (Medtronic, Maastricht, the Netherlands), subsequently, AV block was created by radiofrequency ablation.

After a baseline period of 10 min during which control values were obtained, cAVB dogs were treated with either 0.33 mg/kg/5 min (n = 4) or 0.5 mg/kg/5 min (n = 4) DHE. In separate experiments all dogs were serially challenged with dofetilide (25 μg/kg) to confirm individual arrhythmia susceptibility. When TdP arrhythmias occurred and lasted more than 10–15 s, electrical cardioversion was applied via thoracic paces.

2.2.4. Analysis of in vivo *experiments*

All experiments were performed in chronic AV block conditions, at least 3 weeks after creation of AV block, once electrical remodelling is complete [32]. General anesthesia was induced according to the aforementioned protocol, hereafter; catheters were advanced to RV and LV (the right and left ventricle) respectively in order to record MAP (monophasic action potentials) from the endocardium of the ventricular wall. During all animal experiments standard 6 leads ECG with 4 precordial leads and endocardial LV and RV MAP (precordial ECG leads and RVMAP only in cAVB dogs) were recorded and stored continuously (EPtracer sampling rate 1 kHz, Cardiotek, Maastricht, the Netherlands). Recorded ECG data was analyzed off line using the EPTracer program. RR, QT, PR, and QRS intervals were measured manually at baseline, directly after drug infusion, and every 10 min during the observation periods. For each time point, the displayed intervals represent the average of 5 beats (in rabbits of sinoatrial origin) from the lead that provided the clearest signal (mainly lead II). Monophasic action potential signals were measured semi automatically using Matlab (Mathworks, Natick, USA), values are displayed at 80% repolarization and represent the mean of 30 s recordings [33]. The proarrhythmic marker BVR was quantified as STV from LVMAPD80 as described previously [30]. Note that at some preset time points, ECG intervals could not be obtained from all animals because of arrhythmias, ectopic beats (EB), or conduction disturbances, indicated as not measurable (nm). The occurrence of single and multiple (<4) EB's and number of TdP arrhythmias were scored. TdP was defined as a polymorphic ventricular tachyarrhythmia with at least 5 consecutive undulating QRS complexes with a typical twisting around the isoelectric line of the ECG. Animals were considered inducible if 3 or more TdP episodes occurred in the 10 min observation period.

2.3. Optical action potential measurements in hiPSC-CMs

Cor.4U® hiPSC-CMs (Ncardia, Cologne, Germany) were incubated at 37 °C, 5% CO_2 in Cor.4U® complete human cardiomyocyte culture medium. Before the experiments, the cells were transiently loaded with the voltage-sensitive dye (VSD) FluoVolt (x0.25, for 30 min at room temperature). Afterwards, the medium containing VSD was replaced by fresh serum-free medium (DMEM, Sigma Aldrich, Vienna, Austria). The multi-well plate was placed in an environmentally controlled stage incubator (37 °C, 5% CO2, water-saturated air atmosphere) (Okolab Inc, Burlingame, CA, USA). The FluoVolt fluorescence signal was recorded from a 0.2 × 0.2 mm area using a 40 × (NA 0.6) objective lens. Excitation wavelength was 470 ± 10 nm using a light-emitting diode (LED), and emitted light was collected by photomultiplier (PMT) at 510–560 and. LED, PMT, associated power supplies and amplifiers were supplied by Cairn Research Ltd (Kent, UK). Fluorescence signal was digitized at 10 kHz. Acute effects of drugs were assessed by exposure to studied drug concentration with matched vehicle controls (DMSO). A 20 s recording was then taken 5 min after exposure to the drug or vehicle with only one concentration applied per well. The procedure was repeated five times. The records were subsequently analyzed offline using the pClamp software package v.10.0 (Molecular Devices, Inc., Sunnyvale, CA, USA). APD was measured at 90% repolarization.

2.4. Drugs

For *in vitro* experiments DHE and hortiamine were dissolved in 10 mM DMSO (dimethylsulfoxide, Sigma Aldrich, Vienna, Austria) and diluted in extracellular solutions to the desired concentration. Maximal DMSO concentrations during electrophysiological recordings were 0.1%. For *in vivo* use, DHE was dissolved in DMSO/PEG400/H_2O (2:1:2). Dofetilide was dissolved in 0.1 mol/L HCl (0.1 mg/mL) and diluted in saline to the final concentration. All drug solutions for *in vivo* use were freshly prepared for each experiment.

2.5. Statistics

Data are given as mean ± SEM for *in vitro* studies on mammalian cells, *Xenopus* oocytes and hiPSC-CMs, and as mean ± SD for *in vitro* studies on dog cardiomyocytes and *in vivo* experiments. For within group comparisons, paired sample *t*-test was used. Independent sample *t*-tests were used for group comparisons.

Differences were considered to be significant at $P < 0.05$.

3. Results

3.1. Initial finding

To assess the risk of hERG channel inhibition by medicinal plants, we screened a library of extracts prepared from major herbal drugs of the European and Chinese Pharmacopoeias. A methanolic extract of *Evodia rutaecarpa* was found to induce strong hERG channel inhibition. Application of 100 μg/mL extract to HEK 293 cells stably expressing hERG channels induced 85.2 ± 0.5% (n = 4) inhibition of the potassium current.

The active (hERG blocking) compounds were tracked with an established profiling approach combining HPLC-microfractionation and *in vitro* bioactivity testing [13,34]. Microfractions 13, 14 and 15 inhibited peak tail hERG current by 77.0 ± 13.6% (n = 3), 87.3 ± 3.1% (n = 6) and 87.8 ± 6.8% (n = 3), respectively (black bars in Fig. 1A). Subsequent analysis revealed that the hERG channel inhibitory activity of crude *Evodia* extract was attributable to DHE (**1**) and hortiamine (**3**) (see Fig. 1B).

The effect of DHE and hortiamine on hERG channels was investigated in HEK cells stably expressing hERG channels. Fig. 1C shows the concentration-dependent hERG current inhibition by DHE and hortiamine (1 nM–10 μM) during continuous pulsing at 0.3 Hz. In *Xenopus* oocytes DHE and hortiamine inhibited hERG with IC_{50}s of 6.9 ± 0.8 μM (n = 4) and 4.0 ± 0.7 μM (n = 4), respectively (Fig. S1 in Supplemental Material). Additional studies in *Xenopus* oocytes revealed that resting-state inhibition at 10 μM (DHE: 16.1 ± 6.6%, n = 3 and hortiamine: 34.0 ± 2.8%, n = 3) could be distinguished from additional inhibition of open/inactivated channels during repeated

pulsing (DHE: 46.9 ± 7.4%, n = 3, and hortiamine: 57.4 ± 2.4%, n = 3; Fig. S2 in Supplemental Material). Furthermore, channels recovered insufficiently from block at rest (–100 mV; ~12% for both DHE and hortiamine; see Fig. S2 in Supplemental Material).

3.2. Binding modes of DHE and hortiamine

To gain insight into the molecular mechanism of hERG channel inhibition by DHE and hortiamine, their potential interaction with key amino acids known to interact with hERG blockers [35] was analyzed. For these experiments we made use of mutations Y652A and F656A that are known to reduce the sensitivity of hERG to most hERG inhibitors [36]. The steady-state block by DHE and hortiamine at 300 μM concentrations of hERG channels expressed in *Xenopus* oocytes was significantly reduced for both mutants compared to wild type (WT, see Fig. 2) [36,37].

A molecular docking approach was used to investigate the structural interactions of DHE and hortiamine, whereby an open conformation homology model of the hERG channel was used. The predicted binding modes for DHE and hortiamine are shown in Fig. 3.

Docking suggests that DHE binds to the central cavity of hERG and forms hydrophobic interactions with Y652 and π- π-stacking interactions with the aromatic rings of F656 in segment S6. This binding mode is highly consistent with experimental results (see Fig. 2), and in agreement with previous studies on various hERG blockers [39]. MD simulations were performed to assess the dynamic interactions of DHE and hortiamine with the hERG channel. As shown in Fig. 3C,D the majority of contacts remained the same as described for the original docking. To analyze the interactions of the ligands with the identified binding determinants, distances of the aromatic rings of ligands (indole and ketoquinazoline) and Y652/F656 were measured. Both aromatic rings showed distances to the amino acids between 0.35 and 0.5 nm over time. This range has been described as an important characteristic of π-π stacking interactions [38]. Visual inspection after 40 ns MD simulations showed that the indole ring of DHE was able to arrange itself between Y652 and F656 in a sandwich type manner, thereby allowing π-π stacking interactions with both amino acids (Fig. 3A). These binding interactions exhibited high stability as shown in Fig. 3C. After a short rearrangement of DHE of 6 ns at the beginning of the simulation, the distance of the indole ring to Y652 and F656 was reduced to 0.4 nm, indicating that π-π stacking interactions can occur. Close proximity of the aromatic rings was observed for the rest of the simulation. In the hortiamine simulation comparable π-π stacking interactions were observed.

3.3. DHE in isolated cAVB dog cardiomyocytes

DHE prolonged APD in cAVB cells at 0.01 and 1 μM in a concentration-dependent manner. At higher concentrations (10 μM), APD prolongation was less severe, and the statistical significance compared to baseline values was lost, producing a bell shaped curve (Fig. 4A,B, Table 1).

The increase in STV and the incidence of EADs were also concentration-dependent. While the lowest concentration of 0.01 μM DHE induced EAD in 14% of cells, EAD incidence increased to 100% after application of 1 μM, and decreased to 67% after 10 μM DHE (Fig. 4C, Table 1). APD prolongation, STV increase, and EAD incidence were somewhat lower after dofetilide, a compound that reliably induces EAD's in cAVB cells (Table 1).

3.4. DHE in the anesthetized rabbit

DHE dose dependently affected heart rate, repolarization, and conduction. The low dose of 0.05 mg/kg significantly increased the RR interval and all repolarization parameters (QT 166 ± 19 to 185 ± 21* ms, LVMAPD80 115 ± 12 to 132 ± 20* ms), while conduction parameters (PQ and QRS) remained unaffected (Table 2 upper panels). Administration of the high dose of 0.5 mg/kg 25 min later (when all parameters were back to baseline values; Table 2 lower panels, see control (2) values), increased PQ significantly (69 ± 6 ms to 75 ± 5* ms), and all repolarization parameters increased further (QT 169 ± 21 to 272 ± 63* ms, LVMAPD80 122 ± 15 to 213 ± 40* ms, both $P < 0.05$ vs low dose). The latter culminated in the induction of single ectopic beats (SEB's) (n = 4), multiple ectopic beats (MEB's) (n = 2), and eventually in multiple episodes of TdP in 2/8 rabbits. In accordance, STV values increased significantly beyond the values observed after the low dose of DHE (Table 2).

In the second group of rabbits, the class III agent dofetilide (0.004 mg/kg) increased repolarization to a similar extent as 0.5 mg/kg DHE, but no arrhythmias were observed (Table 2 upper panels). Upon increasing the dose to 0.04 mg/kg (Table 2 lower panels), repolarization parameters increased beyond those seen with either dose of DHE. In addition, QRS duration increased significantly (51 ± 2 to 69 ± 13* ms), and first and second-degree AV block (7/7 and 6/7 rabbits) were observed that were likely the result of excessive QT prolongation [40]. In 2 rabbits SEB's and MEB's were seen, in each of these animals 1 short TdP episode was observed.

3.5. DHE in the proarrhythmic cAVB dog model

Plasma concentrations after i.v. administration of either 0.33 mg/kg or 0.5 mg/kg DHE were determined (Fig. 5).

DHE (0.33 mg/kg) considerably increased repolarization duration (QT + 48 ± 10%*) without affecting conduction (Table 3 upper panels).

This culminated in the development of single and multiple ectopic beats in all animals, and eventually in multiple TdP arrhythmia episodes in 2 dogs (Fig. 6).

In one additional animal a single long-lasting TdP arrhythmia was induced and had to be terminated by electrical cardioversion. In the same animals dofetilide induced a similar increase in repolarization duration (QT + 48 ± 6%*). Also TdP inducibility was similar, with 2/4 dogs showing multiple TdP episodes and one additional animal showing a single non self-terminating TdP arrhythmia.

Administration of 0.5 mg/kg DHE significantly increased QT duration from 382 ± 31 to 577 ± 25* ms (Table 3 lower panels), which was not different from the increases in repolarization duration seen with the lower dose of DHE. Surprisingly, none of the dogs developed TdP (Fig. 7).

In contrast, in 75% of these animals dofetilide was able to reproducibly induce TdP arrhythmias with comparable increases in repolarization parameters.

3.6. Effects of DHE and hortiamine on $Na_V1.5$ and $Ca_V1.2$ channels

Prediction of proarrhythmogenity can be improved by considering the effect of drugs on currents from three key ion channels: hERG, Nav1.5 and Cav1.2 [41]. We have therefore investigated the effects of DHE and hortiamine in HEK cells stably expressing $Na_V1.5$ and transiently expressing $Ca_V1.2$ channels. At the concentration of 10 μM neither DHE nor hortiamine had any effect on sodium (Fig. 8A,B, n = 3) and barium (Fig. 8C,D, n = 3) currents through $Na_V1.5$ and $Ca_V1.2$ channels, respectively.

3.7. Effects of Evodia extracts, DHE and hortiamine on hiPSC-CMs

To evaluate further the proarrhythmic risks, methanolic extracts of *Evodia rutaecarpa* (E1 and E2, see Supplemental Material), DHE and hortiamine were tested in hiPSC-CMs. E1 and E2 significantly

Table 1
DHE and dofetilide in isolated cAVB cardiomyocytes.

		ControlAPD90	'On drug' APD90	%	Control STV	'On drug' STV	EAD
DHE	0.01 μM	370 ± 48	428 ± 86	15 ± 13	16 ± 6	46 ± 54	1/7
	0.1 μM	396 ± 63	555 ± 111[a]	42 ± 29	26 ± 18	121 ± 76[a]	6/9
	1 μM	392 ± 72	636 ± 126[a,b]	69 ± 47	25 ± 17	317 ± 330[b]	11/11
	10 μM	432 ± 57	579 ± 326[c]	36 ± 77	35 ± 32	88 ± 102[c]	4/6
Dofetilide[d]	1 μM	384 ± 111	490 ± 134[a]	38 ± 60	14 ± 10	40 ± 32[a]	15/25

APD90 and STV values are expressed in ms.
[a] $P < 0.05$ vs. control.
[b] APD90 could not be quantified in 7/11 cells because APD >2000 ms.
[c] APD90 could not be quantified in 3/6 cells because APD >2000 ms.
[d] Data from Nalos et al. [29].

Table 2
DHE and dofetilide directly after infusion in normal anesthetized rabbits.

t = 5	Control (1)	DHE (0.05 mg/kg)	%	Control (1)	Dofetilide (0.004 mg/kg)	%
RR	323 ± 52	353 ± 43[a]	10 ± 6	309 ± 37	336 ± 34[a]	9 ± 4
QT	166 ± 19	185 ± 21[a]	12 ± 10[b]	161 ± 15	233 ± 35[a]	46 ± 9
QTc	159 ± 16	171 ± 25[a]	8 ± 8[b]	159 ± 12	221 ± 27[a]	44 ± 9
LVMAP80	115 ± 12	132 ± 20[a]	15 ± 9[b]	116 ± 10	205 ± 20[a]	77 ± 10
JT	113 ± 17	132 ± 19[a]	17 ± 15[b]	110 ± 15	181 ± 36[a]	67 ± 10
PQ	67 ± 7	73 ± 7	9 ± 4	68 ± 6	70 ± 6	1 ± 2
QRS	52 ± 4	54 ± 5	2 ± 3	51 ± 2	52 ± 2	2 ± 3
STV_{LV}	0.4 ± 0.08	0.6 ± 0.2[a]	59 ± 34	0.6 ± 0.2	1.0 ± 0.3[a]	80 ± 78
TdP	0/8	0/8	0	0/7	0/7	0
t = 35	Control (2)	DHE (0.5 mg/kg)	%	Control (2)	Dofetilide[d] (0.04 mg/kg)	%
RR	361 ± 50	421 ± 69[a]	17 ± 13[b]	349 ± 60	726 ± 187[a]	111 ± 56
QT	169 ± 21	272 ± 63[a]	60 ± 26[b,c]	183 ± 19	444 ± 101[a]	140 ± 40
QTc	153 ± 15	240 ± 53[a]	56 ± 26[c]	174 ± 19	322 ± 65[a]	80 ± 25
LVMAP80	122 ± 15	213 ± 40[a]	76 ± 33[b,c]	137 ± 16	380 ± 98[a]	173 ± 56
JT	117 ± 18	214 ± 58[a]	81 ± 36[b,c]	132 ± 20	373 ± 106[a]	176 ± 56
PQ	69 ± 6	75 ± 5[a]	12 ± 2	70 ± 6	nm	nm
QRS	52 ± 4	58 ± 12	12 ± 19	51 ± 2	69 ± 13[a]	35 ± 23
STV_{LV}	0.5 ± 0.8	1.4 ± 0.7[a]	227 ± 252	0.6 ± 0.3	2.6 ± 1.0[a]	393 ± 240
TdP	0/8	2/8	25	0/7	0/7	0

ECG parameters are expressed in ms.
[a] $P < 0.05$ vs control.
[b] $P < 0.05$ vs dofetilide.
[c] $P < 0.05$ vs low dose DHE.
[d] of note: conduction disturbances are present after dofetilide (0.04 mg/kg) treatment.

Table 3
DHE and dofetilide directly after infusion in cAVB dogs.

t = 5 *n = 4*	Control	DHE (0.33 mg/kg)	%	Control	Dofetilide (25 μg/kg)	%
RR	1000	1000	–	1000	1000	–
QT	393 ± 33	581 ± 19[a]	48 ± 10	393 ± 18	582 ± 18[a]	48 ± 6
QRS	118 ± 8	118 ± 7	0.5 ± 2	126 ± 5	127 ± 6	0.4 ± 1
LVMAP80	272 ± 26	430 ± 94	63 ± 48	264 ± 17	399 ± 58[a]	52 ± 28
RVMAP80	247 ± 26	332 ± 14[a]	41 ± 17	253 ± 25	321 ± 25[a]	28 ± 14
STV_{LV}	1.0 ± 0.3	nm (n = 2)	nm	0.8 ± 0.4	2.2 ± 0.3[a]	229 ± 142
TdP	0/4	2/4	50	0/4	2/4	50
MEB	0/4	4/4	100	0/4	4/4	100
SEB	0/4	4/4	100	0/4	4/4	100
t = 5 *n = 4*	Control	DHE (0.5 mg/kg)	%	Control	Dofetilide(25 μg/kg)	%
RR	1000	1000	–	1000	1000	–
QT	382 ± 31	577 ± 25[a]	51 ± 10	408 ± 33	577 ± 36[a]	42 ± 7
QRS	127 ± 9	129 ± 8	2 ± 3	130 ± 5	131 ± 7	1 ± 2
LVMAP80	240 ± 33	356 ± 79[a]	48 ± 20	264 ± 34	344 ± 55[a]	30 ± 5
RVMAP80	234 ± 21	305 ± 37[a]	30 ± 7	242 ± 31	304 ± 63[a]	24 ± 11
STV_{LV}	0.8 ± 0.3	2.0 ± 1.3	144 ± 103	0.9 ± 0.2	4.8 ± 2.4[a]	457 ± 296
TdP	0/4	0/4	0	0/4	3/4	75
MEB	0/4	1/4	25	0/4	3/4	75
SEB	0/4	3/4	73	0/4	4/4	100

ECG parameters are expressed in ms.
TdP, tachycardia with the typical twisting around the isoelectric line of 5 or more beats; MEB < 4 beats.
nm, not measurable due to numerous arrhythmic events.
[a] $P < 0.05$ vs baseline.

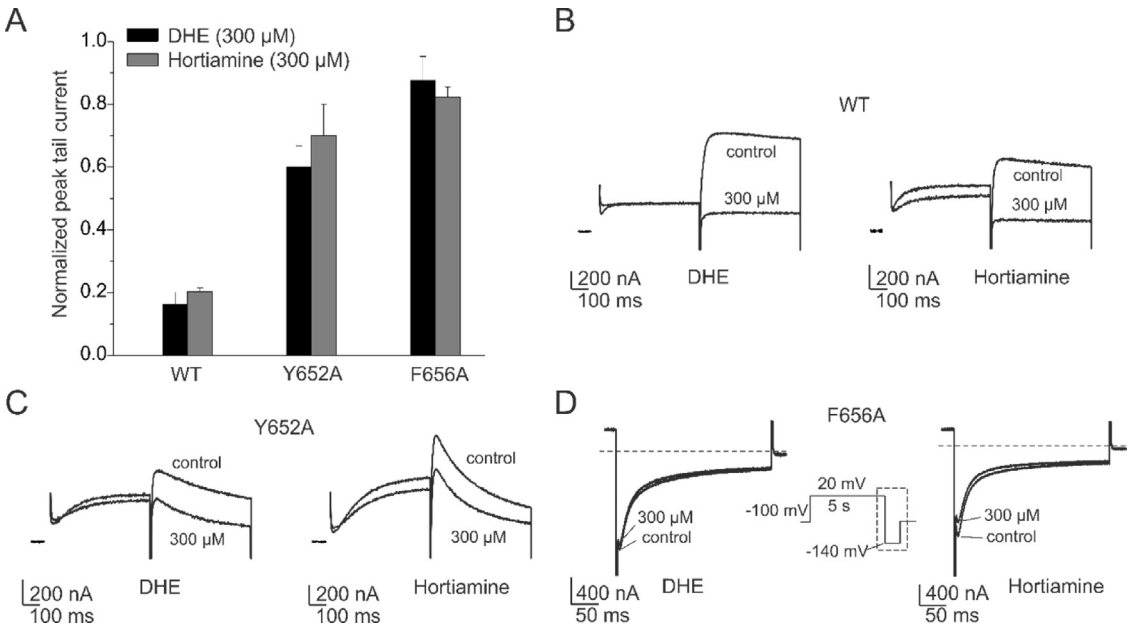

Fig. 2. Inhibition of potassium currents through hERG channels expressed in *Xenopus* oocytes by DHE and hortiamine is suppressed by the inner cavity mutants (Y652A and F656A). (A) The bars display mean normalized peak tail current once steady-state block with 300 μM of DHE (black bars; n = 4 for WT, n = 3 for Y652A and F656A) and hortiamine (grey bars; n = 4 for WT, n = 3 for Y652A and F656A) has been established. The amount of block was significantly ($P < 0.05$) reduced for both mutants compared to WT. (B-D), Representative current traces of wild type and mutant hERG channels in the absence (control) and presence of 300 μM DHE and hortiamine during 0.3 Hz pulse trains. The voltage protocol for WT and Y652A hERG channels is the same as in Fig. 1C. The voltage protocol for F656A mutant is shown as inset in D. Dashed lines represent the zero current level and the box indicates where tail currents have been plotted.

($P < 0.05$) prolonged APD in a concentration-dependent manner from 1 to 100 μg/mL, while at 0.1 μg/mL no significant change in the APD was observed (Fig. 9B, left panel). Maximal APD prolongation was induced by application of 100 μg/mL of E1 and E2 (Fig. 9A,B left panel). DHE and hortiamine prolonged APD in hiPSC-CMs cells in a concentration-dependent manner from 0.01 to 1 μM (Fig. 9B, right panel). APD was significantly ($P < 0.05$) increased for 0.1 and 1 μM compared to control. Hortiamine induced stronger APD prolongation at 1 μM than DHE (Fig. 9A,B right panel). At 3 μM concentration both compounds induced EADs in hiPSC-CMs (Fig. 9C).

4. Discussion and conclusions

Using multiple models (cells, normal rabbits and cAVB dogs) that have been previously used to determine the safety of (non) cardiovascular drugs, we showed that DHE has strong proarrhythmic properties that seem to be self-limiting at higher dosages. The proarrhythmic effects of DHE at the submaximal dose are comparable to dofetilide, an anti-arrhythmic agent known for its proarrhythmic liability.

We identified DHE and hortiamine (Fig. 1) as hERG inhibitors by an approach combining HPLC-microfractionation, patch clamp studies on mammalian cell lines expressing hERG, and on-line and off-line spectroscopic analysis [34,42]. DHE and hortiamine inhibited hERG channels expressed in a mammalian cell line at submicromolar concentrations (IC_{50}(DHE) = 253.2 ± 26.3 nM, n = 4; IC_{50}(hortiamine) = 144.8 ± 35.1 nM, n = 4; Fig. 1C). Channel block in *Xenopus* oocytes occurred at higher concentrations (IC_{50}(DHE) = 6.9 ± 0.8 μM, n = 4; IC_{50}(hortiamine) = 4.0 ± 0.7 μM, n = 4; Fig. S1 in Supplemental Material). This is in line with the commonly observed reduced channel block in *Xenopus* oocytes [43].

hERG channel block by DHE and hortiamine was dramatically reduced by mutations of the two known putative binding determinants on S6 segments (Y652, F656, Fig. 2). Docking suggested that DHE binds to the central cavity of hERG and forms hydrophobic interactions with Y652, and π- π-stacking interactions with the aromatic rings of F656. Furthermore, our data suggest that the indole ring of DHE is able to arrange itself between Y652 and F656 in a sandwich type manner, thereby allowing π-π stacking interactions with both amino acids (Fig. 3).

We subsequently focused on DHE, given that the compound is present in *Evodia* at much higher concentrations than hortiamine [1,34]. DHE concentration-dependently increased repolarization duration in isolated cAVB cardiomyocytes (Fig. 4). Maximum effects were observed using 1 μM DHE, whereby a large increase in repolarization duration and STV was observed, and EAD's were induced in all cells. Compared to literature data for dofetilide, the effect of DHE on repolarization and STV was stronger (Table 1), suggesting at first a comparable or even higher proarrhythmic potential of DHE. However, with 10 μM DHE concentration, APD prolongation, STV increase, and EAD incidence were reduced compared to 1 μM DHE.

In the anesthetized rabbits, repolarization prolongation was the most important electrophysiological effect after 0.05 and 0.5 mg/kg DHE (Table 2). While no arrhythmias were seen after the lower dose of DHE, 0.5 mg/kg DHE induced TdP arrhythmias in 2 out of 8 animals, and STV increased accordingly. Interestingly, despite similar QT prolongation seen with the low dose of the specific I_{Kr} blocker dofetilide (0.004 mg/kg), no arrhythmias were induced. Despite an increase in repolarization parameters beyond those observed with either dose of DHE, also the high dose of dofetilide (0.04 mg/kg) did not induce TdP. The higher STV values seen after administration of this dose were likely due to the presence of AV block which influences the measurements and analysis. However, Kijtawornrat and co-workers observed TdP arrhythmias in 2/10 and 2/6 ketamine-xylazine anesthetized rabbits after administration of a similar dose of dofetilide (0.04 mg/kg/10 min) and another class III agent, clofilium [44]. Similar or higher QT_C values (0.04 mg/kg dofetilide QT_C + ~150 ms; 0.4 mg/kg clofilium QT_C + ~225 ms) were observed compared to dofetilide treated rabbits. In chloralose-anesthetized rabbits similar results were reported. Clofilium (6.0 μmol/kg) and almokalant (78.5 μmol/kg) induced TdP arrhythmias in respectively 3/10 and 1/6 of the animals tested [45,46]. This inconsistency

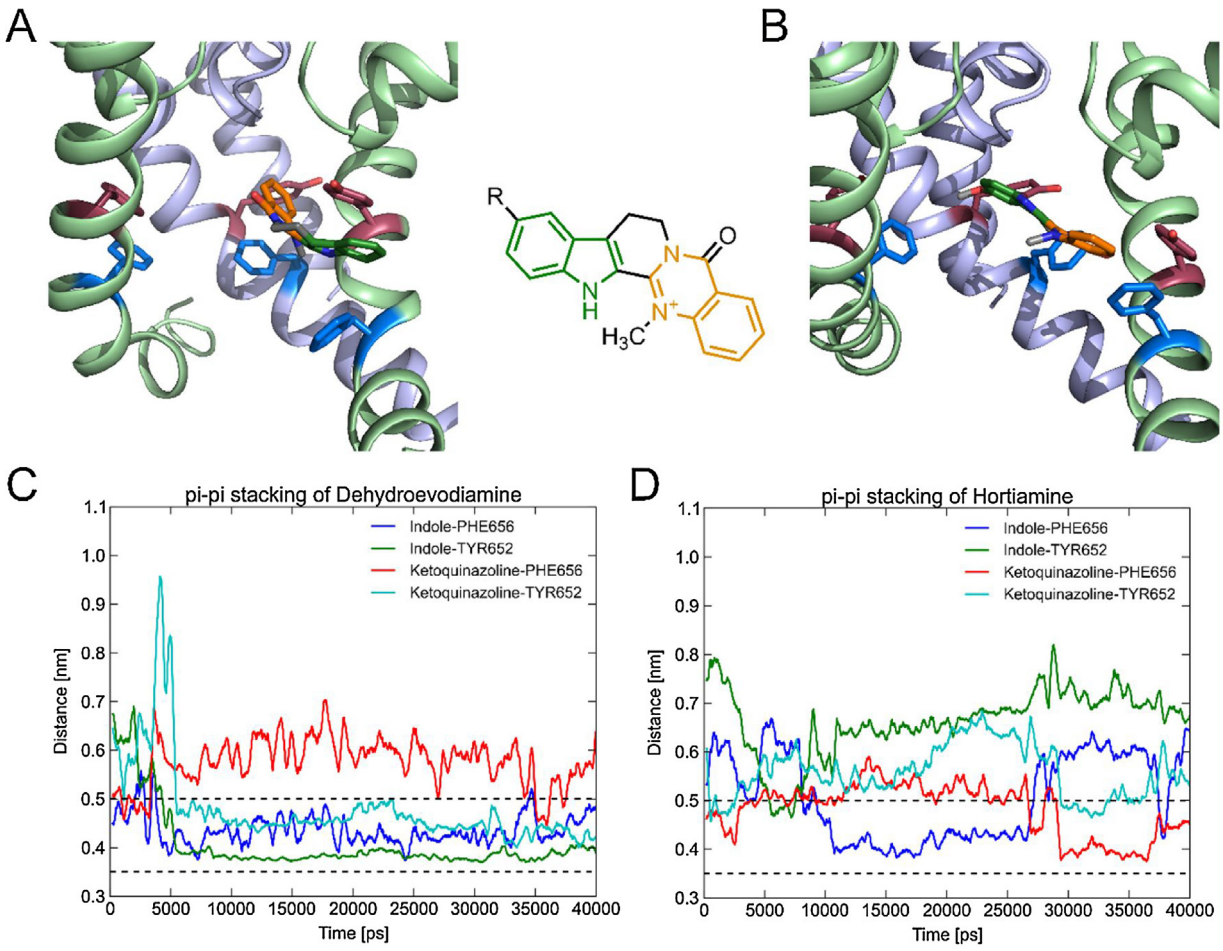

Fig. 3. Docking of DHE and hortiamine within the inner cavity of a homology model of the hERG channel. The drug (A – DHE, B – hortiamine) is shown in green ball and stick representation, and the binding residues Y652 and F656 are shown as blue sticks. The model suggests potential additional interactions with T623 and S624 residues of the selectivity filter. (C, D) MD simulations of DHE and hortiamine, respectively. Distances between aromatic rings are plotted over simulation time. The grey shaded area indicates favorable π-π interactions. Distance cutoffs are taken from Tsuzuki et al. [38].

between QT_C prolongation and TdP incidence with dofetilide and DHE could be due to the limited predictive power of the QT interval regarding induction of arrhythmias [47]. However, regarding the results with class III agents mentioned above, the TdP incidence with dofetilide in our study could be an underestimation. In this case a TdP incidence of 2/8 with 0.5 mg/kg DHE would suggest a proarrhythmic potential similar to several class III compounds and might thus be labeled 'high risk' or 'unsafe' [48].

The dose-dependent proarrhythmic potential of DHE was confirmed in the proarrhythmic cAVB dog model. At a dose of 0.33 mg/kg, which is equivalent to the 0.5 mg/kg dose in rabbits when taking into account the blood volume and body surface area, DHE prolonged repolarization and induced TdP arrhythmia to the same extent as dofetilide (Fig. 6, Table 3 upper panels). Thus, the effects of DHE and dofetilide did not differ. Surprisingly, a moderate increase in dose to 0.5 mg/kg led to similar increases in repolarization duration without an induction of arrhythmias (Fig. 7, Table 3 lower panels). Taking into account the plasma concentrations reached (Fig. 5), 0.33 mg/kg DHE could be considered mainly a hERG/I_{Kr} blocker with minimal or no effect on other cardiac ion currents.

Our *in vitro* and *in vivo* studies revealed for the first time proarrhythmic effects of DHE which is in contrast to previously suggested antiarrhythmic activity [9,49]. According to our findings, the decrease in proarrhythmic potential of the higher dose of 0.5 mg/kg cannot be explained by additional blockage of other ion currents, as we did not observe any block of $Na_V1.5$ and $Ca_V1.2$ channels by DHE and hortiamine at 10 μM (Fig. 8; but see data from different assays [8,9,49]). Moreover, we did not observe QRS interval widening or negative inotropic effects, which may also speak against blockage of these ion currents. However, extra cardiac effects cannot be excluded. These self-limiting electrophysiological properties of DHE are not unique, as they have been already shown for cisapride and vernakalant [31].

The use of iPSC-CMs in drug safety studies has been proposed by the Food and Drug Administration (FDA) in frame of the "Comprehensive *in vitro* Proarrhythmia Assay" (CiPA) initiative as suitable *in vitro* model for evaluation of the drug proarrhythmic risks [50]. We therefore investigated the effects of Evodia extracts, DHE and hortiamine on APD in hiPSC-CMs. The concentration-dependent APD prolongation was confirmed for two methanolic extracts (Fig. 9A,B, left panel) prepared from *E. rutaecarpa* fruits that were purchased from the different suppliers (see Supplemental Materials). DHE and hortiamine also prolonged APD in hiPSC-CMs cells in a concentration-dependent manner from 0.01 to 1 μM and induced EADs at 3 μM (Fig. 9A,B, right panel, C). In line with the more potent hERG channel inhibition (Fig. 1 and Fig. S1) hortiamine induced stronger APD prolongation at 1 μM than DHE.

Interestingly, the observed plasma levels of 0.383 ± 0.057 μg/mL and 0.710 ± 0.106 μg/mL after intravenous

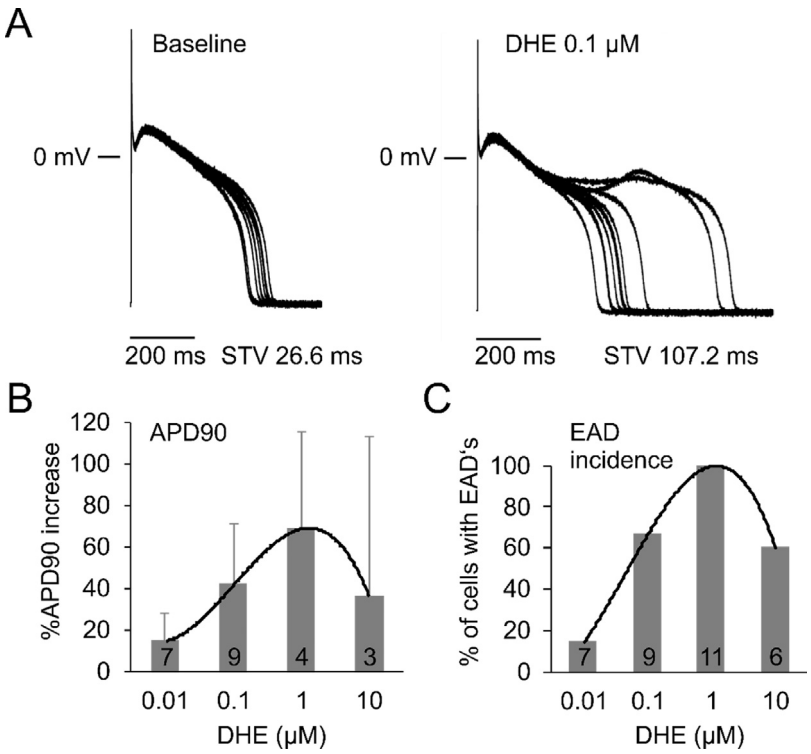

Fig. 4. DHE effects on APD and EAD incidence in cAVB cells. (A) Compared to baseline (left panel), 0.1 μM DHE induced a pronounced prolongation of the action potential (right panel). Furthermore, EADs become apparent, which are preceded by a pronounced increase in STV. (B, C) The bar graphs represent APD90 increase and EAD incidence observed with each tested DHE concentration. Note that, due to decrease of both parameters at higher dosages, a bell-shaped curve appears. Numbers within bars indicate the number of cells. APD90 was significantly ($P < 0.05$) increased for 0.1 and 1 μM DHE compared to control. In contrast to EAD incidence, APD90 could not be determined in 7/11 cells at 1 μM and 3/6 cells at 10 μM due to APD >2000 ms (pacing at 0.5 Hz).

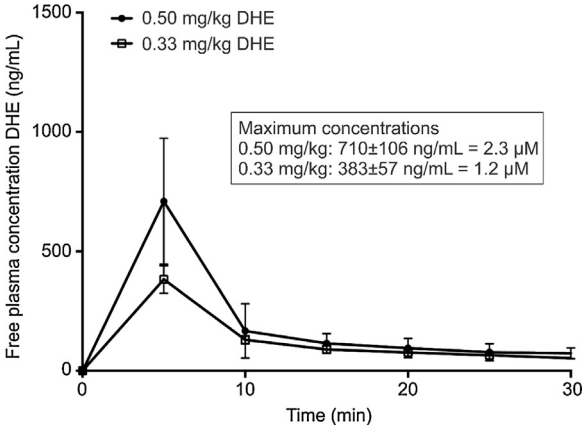

Fig. 5. DHE plasma concentration in cAVB dogs. The graph displays the plasma concentration of DHE after i.v. administration of 0.33 (n = 4) and 0.5 mg/kg DHE (n = 3). Maximal plasma concentrations (1.2–2.3 μM) are reached 5 min after administration.

administration of 0.33 or 0.5 mg/kg DHE (Fig. 5), respectively, are in the range of plasma levels found after oral administration of 100 (0.4 ± 0.1 μg/mL) or 500 mg/kg (1.7 ± 0.3 μg/mL) DHE to rats [51]. Furthermore, oral administration of the herbal drug Wu-Zhu-Yu (Evodiae fructus) to rats yielded similar (0.564 ± 0.246 μg/mL) [52] or higher (7.64 ± 0.63 μg/mL) [53] DHE plasma levels depending on the dose given. However, plasma levels in humans after ingestion of Wu-Zhu-Yu (prepared and dosed according to Chinese standards) are not known at present.

The oral bioavailability of DHE was demonstrated in several pharmacokinetic studies in rats which received either the pure compound or an *Evodia* preparation by intragastric administration [51,53–55]. Lin et al. [51] reported that the oral bioavailability of DHE was approximately 15%, and protein binding was 65%. In an intestinal absorption model with Caco-2 cells, DHE permeated the monolayer without any directional preference, gave additional evidence for intestinal absorption [54].

From a consumer safety perspective and in view of clinical implications, quantitative data on the DHE content in commercially available *Evodia* preparations seemed of particular interest. The content of DHE in various *Evodia* products were previously determined and the amount in recommended daily doses calculated [56]. DHE was detected in all herbal drug and finished products (extract granules commercially available in Europe), but quantitative differences were observed between the products. Overall, the possible daily intake from crude drugs appeared significantly higher than from processed *Evodia*-containing products. Although we found prolongation of repolarization by DHE, hortiamine and Evodia exctracts in hiPSC-CMs, and prolongation of repolarization and TdP arrhythmias induced by concentrations of DHE that might be clinically relevant in dogs, these results cannot be directly extrapolated to the herbal drug itself, or to *Evodia*-containing finished TCM products. The herbal drug may contain compounds that can either potentiate or counteract the proarrhythmic effects of DHE and hortiamine, or that may affect, positively or negatively, its bioavailability. Our study focused on DHE as the major hERG blocking compound identified in *Evodia* extract.

In summary, data from a combination of patch clamp on mammalian cell lines expressing hERG, $Na_V1.5$ and $Ca_V1.2$ channels, microelectrode studies on dog ventricular cardiomyocytes, optical AP measurements in hiPSC-CMs and *in vivo* studies on two animal models (rabbit and cAVB dog) suggest a cardiac safety risk associated with the intake of DHE, hortiamine and herbal drugs containing them. Despite the wide use of *Evodia* no data on human

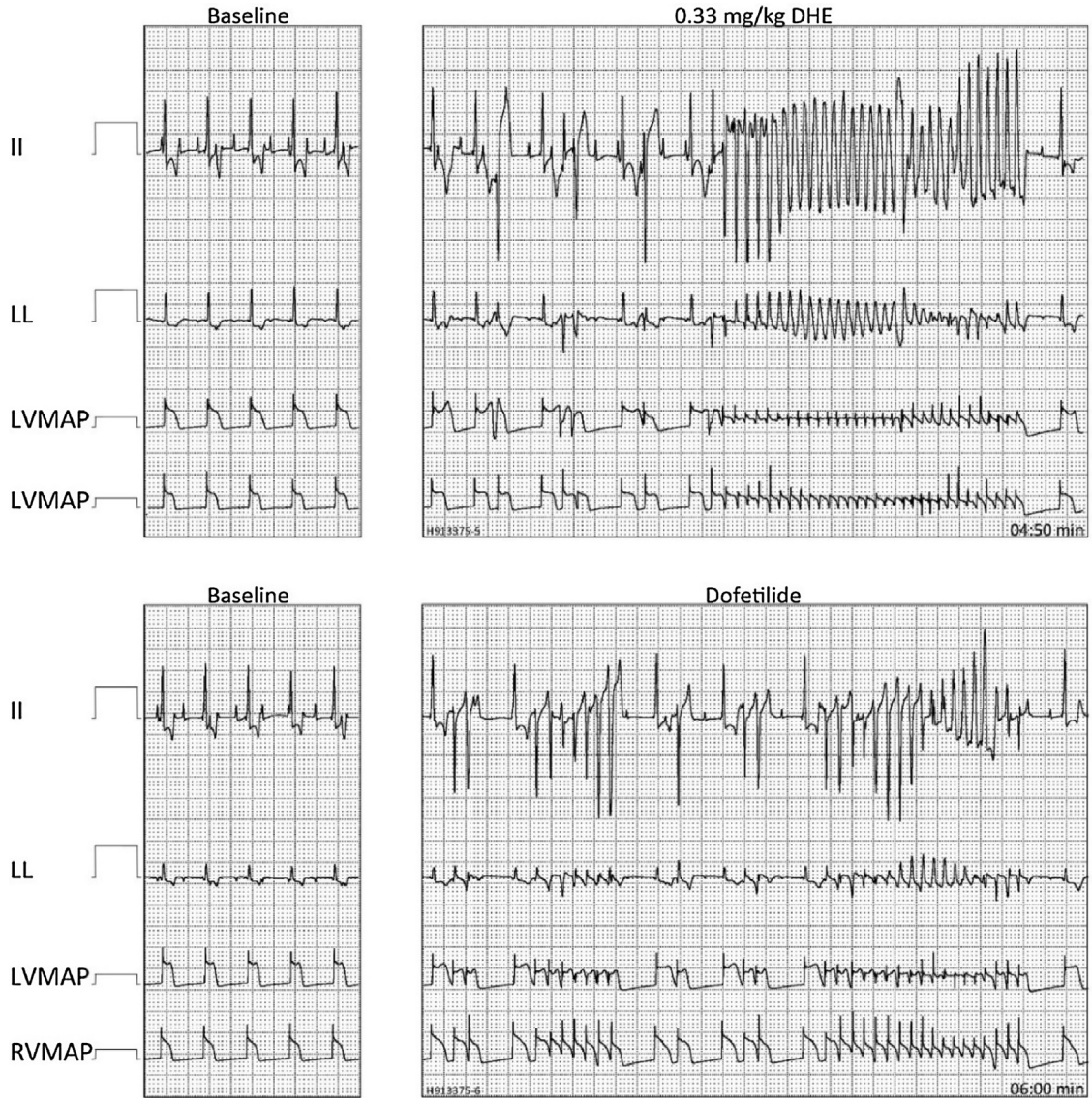

Fig. 6. Proarrhythmic effects of 0.33 mg/kg DHE and dofetilide. Two ECG leads (II an LL) and LV and RV MAP recording are shown from the same dog after 0.33 mg/kg DHE (upper panels), and after challenge with dofetilide (lower panels). Calibration bars represent 1 s (width) and 10 mV (height) for the surface ECG, and 1 s (width) and 5 mV (height) for the MAP signals. In both instances prolongation of the parameters representing repolarization and induction of TdP are observed.

plasma levels of DHE and hortiamine are currently available. Our study should increase awareness of possible proarrhythmic effects, and warrant future investigations, such as QT measurements in humans taking *Evodia* extracts and concomitant analysis of plasma levels of DHE and hortiamine. From a consumer safety perspective, the case of *Evodia* products and DHE shows that investigations into possible hERG liabilities and cardiac safety of other herbal products, in particular alkaloid-containing herbal drugs, are needed.

Funding

This work was supported by the Austrian Science Fund (FWF) [grant number W1232 to SH]; Austrian Science Fund (FWF) [grant number P27729 to SB]; the Swiss National Science Foundation grant number 205320_126888 to MHa]; and European Community's Seventh Frame Program FP7/2007-2013 [grant number HEALTH-F2-2009-241526EUTrigTreat (R.V. Utrecht)].

Author contributions

IB designed the study, wrote the manuscript, performed and analyzed voltage and patch clamp experiments (hERG, $Na_V1.5$), contributed to dog CMs and hiPSC-CMs experiments; RV carried out and analyzed *in vivo* experiments and wrote the manuscript; AS performed preparative purification and identification of DHE and hortiamine, and quantitative analysis of *Evodia* crude drug and *Evodia*-containing products; PSa contributed to dog CMs experiments; SB performed and analyzed patch clamp experiments ($Ca_V1.2$); PSz performed patch clamp ($Na_V1.5$) and hiPSC-CMs experiments; TL performed MD simulations and docking studies; AS-W performed MD simulations and docking studies, and was involved in writing the manuscript; MAGH designed the study and wrote the manuscript; MHo. carried out and analyzed cardiomyocyte experiments; HT carried out and analyzed cardiomyocyte experiments; MJ carried out and analyzed cardiomyocyte experiments; JHDB carried out in vivo experiments; MHa developed the process for preparative purification of DHE and hortiamine, and

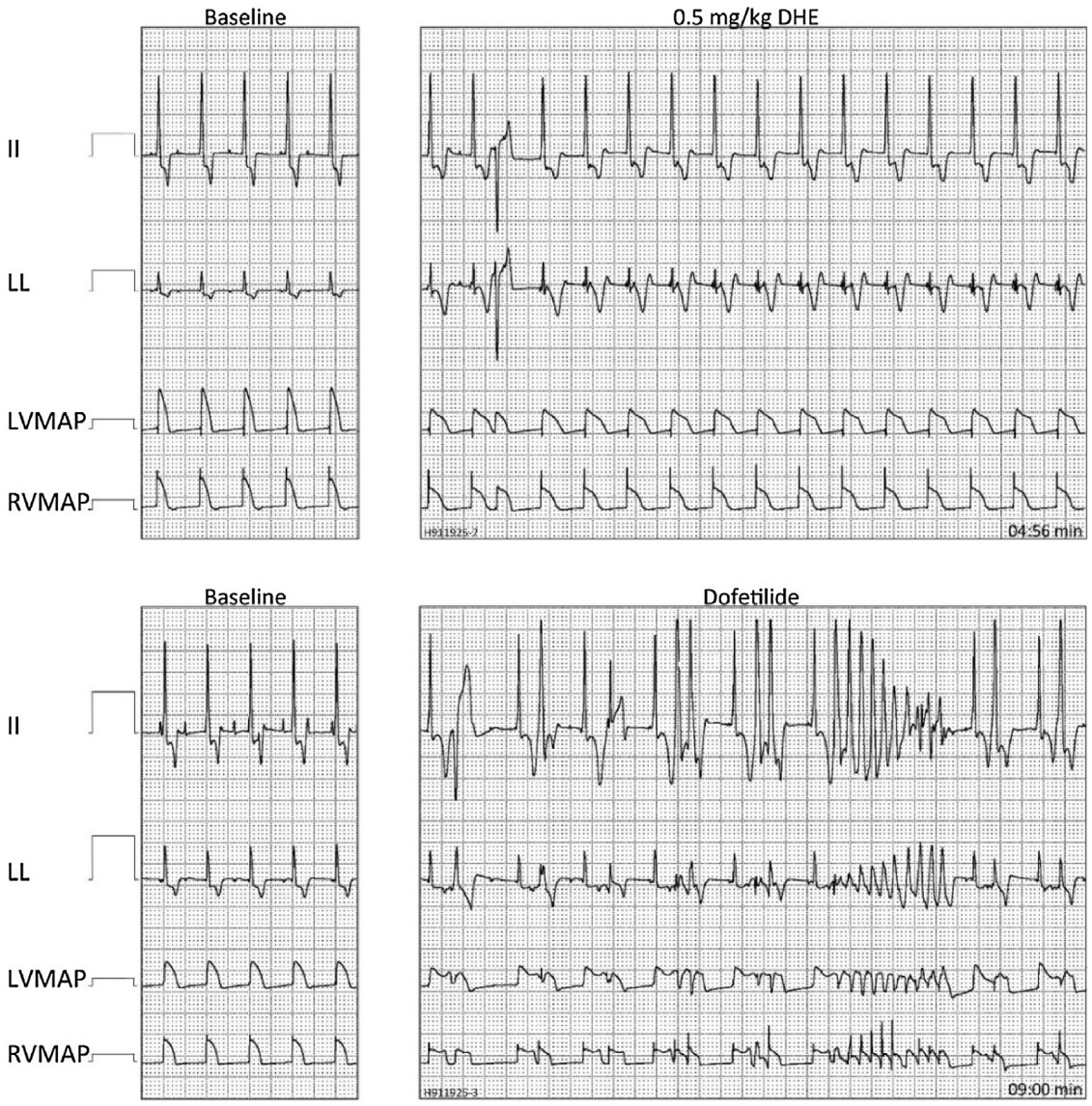

Fig. 7. Proarrhythmic effects of 0.5 mg/kg DHE and dofetilide. Two ECG leads (II an LL) and LV and RV MAP recording are shown from the same dog after 0.5 mg/kg DHE (upper panels), and after challenge with dofetilide (lower panels). Calibration bars represent 1 s (width) and 10 mV (height) for the surface ECG, and 1 s (width) and 5 mV (height) for the MAP signals. DHE (0.5 mg/kg) does not induce TdP with similar lengthening of repolarization intervals as dofetilide.

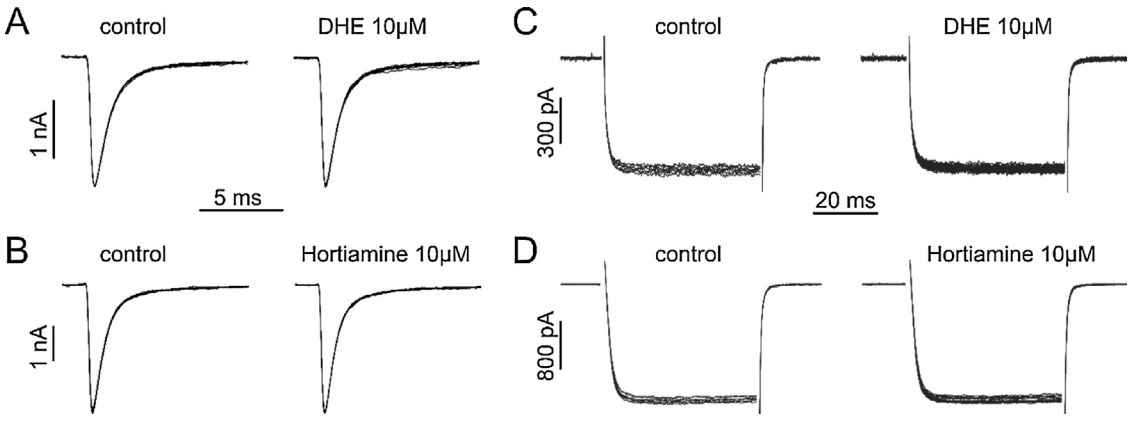

Fig. 8. No effect of DHE and hortiamine on $Na_V1.5$ and $Ca_V1.2$ channels. Superimposed sodium currents during a train of 10 ms pulses (0.2 Hz) in absence of drug (control) and after application of DHE (10 μM, A) and hortiamine (10 μM, B). Superimposed barium currents during a train of 50 ms pulses (0.2 Hz) in absence of drug (control) and after application of DHE (10 μM, C) and hortiamine (10 μM, D).

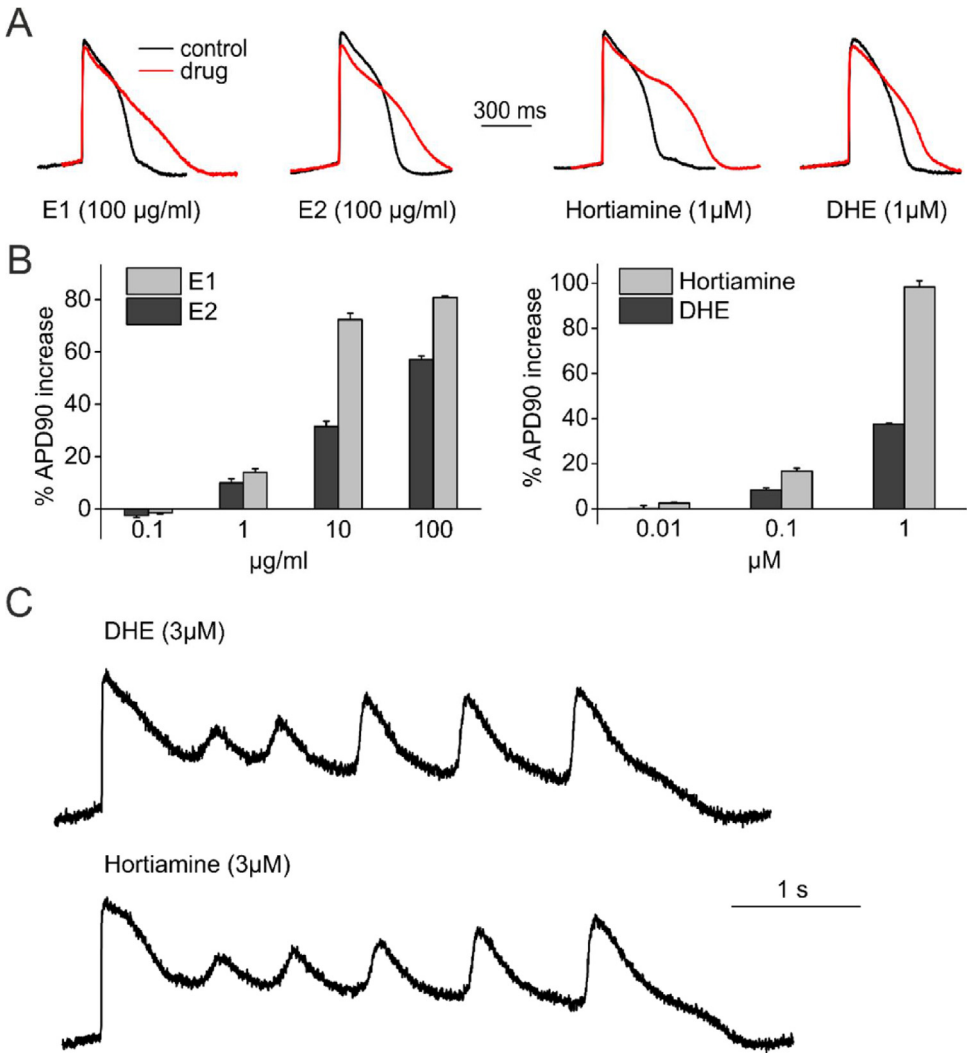

Fig. 9. Effects of Evodia extracts, DHE and hortiamine on APD in hiPSC-CMs. (A) Mean AP recordings in control (black) and after 5 min incubation in drug (red) at the indicated concentration. (B) The bar graphs represent APD90 increase observed with each tested concentration of E1 and E2 (n = 5, left panel) and DHE and hortiamine (n = 5, right panel). (C) Represenative AP recordings illustrating occurrence of the EADs after 5 min incubation in DHE and hortiamine (3 µM).

was involved in writing the manuscript; MAV designed the study and wrote the manuscript; SH designed the study and wrote the manuscript.

Conflict of interest

None.

Appendix A. Supplementary data

Supplementary data associated with this article can be found, in the online version, at https://doi.org/10.1016/j.phrs.2018.02.024.

References

[1] W. Tang, G. Eisenbrand, Handbook of Chinese Medicinal Plants – Chemistry, Pharmacology, Toxicology, Wiley-VCH Verlag, 2011.
[2] Food and Drug Administration, HHS, International Conference on Harmonisation; guidance on S7A safety pharmacology studies for human pharmaceuticals; availability. Notice, Fed Regist. 66 (2001) 36791–36792.
[3] Food and Drug Administration, HHS, International Conference on Harmonisation; guidance on S7B Nonclinical Evaluation of the Potential for Delayed Ventricular Repolarization (QT Interval Prolongation) by Human Pharmaceuticals; availability. Notice, Fed Regist. 70 (2005) 61133–61134.
[4] J.L. Vanherweghem, C. Tielemans, D. Abramowicz, M. Depierreux, R. Vanhaelen-Fastre, M. Vanhaelen, M. Dratwa, C. Richard, D. Vandervelde, D. Verbeelen, M. Jadoul, Rapidly progressive interstitial renal fibrosis in young women: association with slimming regimen including Chinese herbs, Lancet 341 (1993) 387–391.
[5] W.F. Chiou, J.F. Liao, A.Y.C. Shum, C.F. Chen, Mechanisms of vasorelaxant effect of dehydroevodiamine: a bioactive isoquinazolinocarboline alkaloid of plant origin, J. Cardiovasc. Pharm. 27 (1996) 845–853.
[6] H.Y. Yang, S.Y. Li, C.F. Chen, Hypotensive effects of dehydroevodiamine, a quinazolinocarboline alkaloid isolated from evodiae-rutaecarpa, Asia Pac. J. Pharmacol. 3 (1988) 191–196.
[7] M.C.M. Yang, S.L. Wu, J.S. Kuo, C.F. Chen, The hypotensive and negative chronotropic effects of dehydroevodiamine, Eur. J. Pharmacol. 182 (1990) 537–542.
[8] C.I. Lin, S.H. Loh, H.N. Luk, W.M. Lue, C.F. Chen, Electropharmacological effects of Dehydroevodiamine on mammalian hearts, J. Chin. Med. 1 (1990) 84–93.
[9] S.H. Loh, A.R. Lee, W.H. Huang, C.I. Lin, Ionic mechanisms responsible for the antiarrhythmic action of dehydroevodiamine in guinea-pg isolated cardiomyocytes, Br. J. Pharmacol. 106 (1992) 517–523.
[10] M.C. Sanguinetti, M. Tristani-Firouzi, HERG potassium channels and cardiac arrhythmia, Nature 440 (2006) 463–469, http://dx.doi.org/10.1038/nature04710.
[11] A. Dennis, L. Wang, X. Wan, E. Ficker, HERG channel trafficking: novel targets in drug induced long QT syndrome, Biochem. Soc. Trans. 35 (2007) 1060–1063, http://dx.doi.org/10.1042/BST0351060.
[12] J.C. Hancox, M.J. McPate, A. El Harchi, Y.H. Zhang, The hERG potassium channel and hERG screening for drug-induced torsades de pointes, Pharmacol. Ther. 119 (2008) 118–132, http://dx.doi.org/10.1016/j.pharmthera.2008.05.009.

[13] G. Gintant, An evaluation of hERG current assay performance: translating preclinical safety studies to clinical QT prolongation, Pharmacol. Therapeut. 129 (2011) 109–119, http://dx.doi.org/10.1016/j.pharmthera.2010.08.008.
[14] J.M. Kratz, D. Schuster, M. Edtbauer, P. Saxena, C.E. Mair, J. Kirchebner, B. Matuszczak, I. Baburin, S. Hering, J.M. Rollinger, Experimentally validated HERG pharmacophore models as cardiotoxicity prediction tools, J. Chem. Inf. Model. 54 (2014) 2887–2901, http://dx.doi.org/10.1021/ci5001955.
[15] S.M. Iqbal, R. Lemmens-Gruber, Voltage gated ion channels blockade is the underlying mechanism of BIMU8 induced cardiotoxicity, Toxicol. Lett. 277 (2017) 64–68, http://dx.doi.org/10.1016/j.toxlet.2017.05.024.
[16] C. Farre, A. Haythornthwaite, C. Haarmann, S. Stoelzle, M. Kreir, M. George, A. Brüggemann, N. Fertig, Port-a-patch and patchliner: high fidelity electrophysiology for secondary screening and safety pharmacology, Comb. Chem. High Throughput Screen. 12 (2009) 24–37.
[17] L. Polonchuk, Toward a new gold standard for early safety: automated temperature-controlled hERG test on the patchliner, Front. Pharmacol. 3 (2012) 3, http://dx.doi.org/10.3389/fphar.2012.00003.
[18] S. Beyl, K. Depil, A. Hohaus, A. Stary-Weinzinger, T. Linder, E. Timin, S. Hering, Neutralisation of a single voltage sensor affects gating determinants in all four pore-forming S6 segments of Ca(V)1.2: a cooperative gating model, Pflugers Arch. 464 (2012) 391–401, http://dx.doi.org/10.1007/s00424-012-1144-5.
[19] A. Windisch, E. Timin, T. Schwarz, D. Stork-Riedler, T. Erker, G. Ecker, S. Hering, Trapping and dissociation of propafenone derivatives in HERG channels, Br. J. Pharmacol. 162 (2011) 1542–1552, http://dx.doi.org/10.1111/j.1476-5381.2010.01159.x.
[20] A. Stary, S.J. Wacker, L. Boukharta, U. Zachariae, Y. Karimi-Nejad, J. Aqvist, G. Vriend, B.L. de Groot, Toward a consensus model of the HERG potassium channel, ChemMedChem 5 (2010) 455–467, http://dx.doi.org/10.1002/cmdc.200900461.
[21] B. Hess, C. Kutzner, D. van der Spoel, E. Lindahl, GROMACS 4: algorithms for highly efficient, load-balanced, and scalable molecular simulation, J. Chem. Theory Comput. 4 (2008) 435–447, http://dx.doi.org/10.1021/ct700301q.
[22] K. Knape, T. Linder, P. Wolschann, A. Beyer, A. Stary-Weinzinger, In silico analysis of conformational changes induced by mutation of aromatic binding residues: consequences for drug binding in the hERG K+ channel, PLoS One 6 (2011) e28778, http://dx.doi.org/10.1371/journal.pone.0028778.
[23] M.G. Wolf, M. Hoefling, C. Aponte-Santamaría, H. Grubmüller, G. Groenhof, g_membed: efficient insertion of a membrane protein into an equilibrated lipid bilayer with minimal perturbation, J. Comput. Chem. 31 (2010) 2169–2274, http://dx.doi.org/10.1002/jcc.21507.
[24] V. Hornak, R. Abel, A. Okur, B. Strockbine, A. Roitberg, C. Simmerling, Comparison of multiple Amber force fields and development of improved protein backbone parameters, Proteins 65 (2006) 712–725, http://dx.doi.org/10.1002/prot.21123.
[25] O. Berger, O. Edholm, F. Jahnig, Molecular dynamics simulations of a fluid bilayer of dipalmitoylphosphatidylcholine at full hydration, constant pressure, and constant temperature, Biophys. J. 72 (1997) 2002–2013, http://dx.doi.org/10.1016/S0006-3495(97)78845-3.
[26] W.L. Jorgensen, J. Chandrasekhar, J.D. Madura, R.W. Impey, M.L. Klein, Comparison of simple potential functions for simulating liquid water, J. Chem. Phys. 79 (1983) 926, http://dx.doi.org/10.1063/1.445869.
[27] M.J. Frisch, G.W. Trucks, H.B. Schlegel, G.E. Scuseria, M.A. Robb, J.R. Cheeseman, G. Scalmani, V. Barone, B. Menucci, G.A. Petersson, H. Nakatsuji, M. Caricato, X. Li, H. Hratchian, A.F. Izmaylov, J. Bloino, G. Zheng, J.L. Sonnenberg, M. Hada, M. Ehara, K. Toyota, R. Fukuda, J. Hasegawa, M. Ishida, T. Nakajima, Y. Honda, O. Kitao, H. Nakai, T. Vreven, J.A. Montgomery Jr., J.E. Peralta, F. Ogliaro, M. Bearpark, J.J. Heyd, E. Brothers, K.N. Kudin, V.N. Staroverov, R. Kobayashi, J. Normand, K. Raghavachari, A. Rendell, J.C. Burant, S.S. Iyengar, J. Tomasi, M. Cossi, N. Rega, J.M. Millam, M. Klene, J.E. Knox, J.B. Cross, V. Bakken, C. Adamo, J. Jaramillo, R. Gomperts, R.E. Stratmann, O. Yazyev, A.J. Austin, R. Cammi, C. Pomelli, J.W. Ochterski, R.L. Martin, K. Morokuma, V.G. Zakrzewski, G.A. Voth, P. Salvador, J.J. Dannenberg, S. Dapprich, A.D. Daniels, Farkas Ö, J.B. Foresman, J.V. Ortiz, J. Cioslowski, D.J. Fox, GAUSSIAN 09, Revision A.1, Gaussian, Inc., Wallingford CT, 2009.
[28] D.A. Case, T.A. Darden, T.E. Cheatham, C.L. Simmerling, J. Wang, R.E. Duke, R. Luo, R.C. Walker, W. Zhang, K.M. Merz, B. Roberts, B. Wang, S. Hayik, A. Roitberg, G. Seabra, I. Kolossváry, K.F. Wong, F. Paesani, J. Vanicek, J. Liu, X. Wu, S.R. Brozell, T. Steinbrecher, H. Gohlke, Q. Cai, X. Ye, J. Wang, M.J. Hsieh, G. Cui, D.R. Roe, D.H. Mathews, M.G. Seetin, C. Sagui, V. Babin, T. Luchko, S. Gusarov, A. Kovalenko, P.A. Kollman, Amber 11, University of California, San Francisco, 2010.
[29] L. Nalos, R. Varkevisser, M.K. Jonsson, M.J. Houtman, J.D. Beekman, R. van der Nagel, M.B. Thomsen, G. Duker, P. Sartipy, T.P. de Boer, M. Peschar, M.B. Rook, T.A. van Veen, M.A. van der Heyden, M.A. Vos, Comparison of the IKr blockers moxifloxacin, dofetilide and E-4031 in five screening models of pro-arrhythmia reveals lack of specificity of isolated cardiomyocytes, Br. J. Pharmacol. 165 (2012) 467–478, http://dx.doi.org/10.1111/j.1476-5381.2011.01558.x.
[30] M.B. Thomsen, S.C. Verduyn, M. Stengl, J.D. Beekman, G. de Pater, J. van Opstal, P.G. Volders, M.A. Vos, Increased short-term variability of repolarization predicts d-sotalol-induced torsades de pointes in dogs, Circulation 110 (2004) 2453–2459, http://dx.doi.org/10.1161/01.CIR.0000145162.64183.C.
[31] R. Varkevisser, M.A. van der Heyden, R.G. Tieland, J.D. Beekman, M.A. Vos, Vernakalant is devoid of proarrhythmic effects in the complete AV block dog model, Eur. J. Pharmacol. 720 (2013) 49–54, http://dx.doi.org/10.1016/j.ejphar.2013.10.054.
[32] M. Schoenmakers, C. Ramakers, J.M. van Opstal, J.D. Leunissen, C. Londono, M.A. Vos, Asynchronous development of electrical remodeling and cardiac hypertrophy in the complete AV block dog, Cardiovasc. Res. 59 (2003) 351–359, http://dx.doi.org/10.1016/S0008-6363(03)00430-9.
[33] A. Dunnink, J.M. van Opstal, P. Oosterhoff, S.K. Winckels, J.D. Beekman, R. van der Nagel, S. Cora Verduyn, M.A. Vos, Ventricular remodelling is a prerequisite for the induction of dofetilide-induced torsade de pointes arrhythmias in the anaesthetized, complete atrio-ventricular-block dog, Europace 14 (2012) 431–436, http://dx.doi.org/10.1093/europace/eur311.
[34] A. Schramm, I. Baburin, S. Hering, M. Hamburger, HERG channel inhibitors in extracts of Coptidis rhizoma, Planta Med. 77 (2011) 692–697, http://dx.doi.org/10.1055/s-0030-1270920.
[35] M. Perry, M. Sanguinetti, J. Mitcheson, Revealing the structural basis of action of hERG potassium channel activators and blockers, J. Physiol. 588 (2010) 3157–3167, http://dx.doi.org/10.1113/jphysiol.2010.194670.
[36] J.S. Mitcheson, J. Chen, M. Lin, C. Culberson, M.C. Sanguinetti, A structural basis for drug-induced long QT syndrome, Proc. Natl. Acad. Sci. U. S. A. 97 (2000) 12329–12333, http://dx.doi.org/10.1073/pnas.210244497.
[37] S.L. Cockerill, J.S. Mitcheson, Direct block of human ether-a-go-go-related gene potassium channels by caffeine, J. Pharmacol. Exp. Ther. 316 (2006) 860–868, http://dx.doi.org/10.1124/jpet.105.094755.
[38] S. Tsuzuki, K. Honda, R. Azumi, Model chemistry calculations of thiophene dimer interactions: origin of pi-stacking, J. Am. Chem. Soc. 124 (2002) 12200–12209.
[39] D. Stork, E.N. Timin, S. Berjukow, C. Huber, A. Hohaus, M. Auer, S. Hering, State dependent dissociation of hERG channel inhibitors, Br. J. Pharmacol. 151 (2007) 1368–1376, http://dx.doi.org/10.1038/sj.bjp.0707356.
[40] R. Varkevisser, M.A. Vos, J.D. Beekman, R.G. Tieland, M.A.G. Van der Heyden, AV-block and conduction slowing prevail over TdP arrhythmias in the methoxamine-sensitized pro-arrhythmic rabbit model, J. Cardiovasc. Electrophysiol. 26 (2015) 82–89, http://dx.doi.org/10.1111/jce.12533.
[41] J. Kramer, C.A. Obejero-Paz, G. Myatt, Y.A. Kuryshev, A. Bruening-Wright, J.S. Verducci, A.M. Brown, MICE models: superior to the HERG model in predicting Torsade de Pointes, Sci. Rep. 3 (2013) 2100, http://dx.doi.org/10.1038/srep02100.
[42] O. Potterat, M. Hamburger, Combined use of extract libraries and HPLC-based activity profiling for lead discovery: potential, challenges, and practical considerations, Planta Med. 80 (2014) 1171–3181, http://dx.doi.org/10.1055/s-0034-1382900.
[43] A.L. Goldin, in: J.J. Clare, D.J. Trezise (Eds.), Expression and Analysis of Recombinant Ion Channels: From Structural Studies to Pharmacological Screening, Wiley–VCH Verlag, Weinheim, Germany, 2006, pp. 1–25.
[44] A. Kijtawornrat, Y. Nishijima, B.M. Roche, B.W. Keene, R.L. Hamlin, Use of a failing rabbit heart as a model to predict torsadogenicity, Toxicol. Sci. 93 (2006) 205–212, http://dx.doi.org/10.1093/toxsci/kfl025.
[45] L. Carlsson, O. Almgren, G. Duker, QTU-prolongation and torsades de pointes induced by putative class III antiarrhythmic agents in the rabbit: etiology and interventions, J. Cardiovasc. Pharmacol. 16 (1990) 276–285.
[46] L. Carlsson, C. Abrahamsson, B. Andersson, G. Duker, G. Schiller-Linhardt, Proarrhythmic effects of the class III agent almokalant: importance of infusion rate, QT dispersion, and early afterdepolarisations, Cardiovasc. Res. 27 (1993) 2186–2193.
[47] R. Varkevisser, S.C. Wijers, M.A. van der Heyden, J.D. Beekman, M. Meine, M.A. Vos, Beat-to-beat variability of repolarization as a new biomarker for proarrhythmia in vivo, Heart Rhythm. 9 (2012) 1718–1726, http://dx.doi.org/10.1016/j.hrthm.2012.05.016.
[48] L. Carlsson, The anaesthetised methoxamine-sensitised rabbit model of torsades de pointes, Pharmacol. Ther. 119 (2008) 160–167, http://dx.doi.org/10.1016/j.pharmthera.2008.04.004.
[49] S.H. Loh, Y.T. Tsai, C.Y. Lee, C.Y. Chang, C.S. Tsai, T.H. Cheng, C.I. Lin, Antiarrhythmic effects of dehydroevodiamine in isolated human myocardium and cardiomyocytes, J. Ethnopharmacol. 153 (2014) 753–762, http://dx.doi.org/10.1016/j.jep.2014.03.043.
[50] C.L. Lei, K. Wang, M. Clerx, R.H. Johnstone, M.P. Hortigon-Vinagre, V. Zamora, A. Allan, G.L. Smith, D.J. Gavaghan, G.R. Mirams, L. Polonchuk, Tailoring mathematical models to stem-cell derived cardiomyocyte lines can improve predictions of drug-induced changes to their electrophysiology, Front. Physiol. 8 (2017) 986, http://dx.doi.org/10.3389/fphys.2017.00986.
[51] L.C. Lin, S.H. Li, Y.T. Wu, K.L. Kuo, T.H. Tsai, Pharmacokinetics and urine metabolite identification of dehydroevodiamine in the rat, J. Agric. Food Chem. 60 (2012) 1595–1604, http://dx.doi.org/10.1021/jf204365m.
[52] H. Xu, Q. Li, Y. Yin, C. Lv, W. Sun, B. He, R. Liu, X. Chen, K. Bi, Simultaneous determination of three alkaloids, four ginsenosides and limonin in the plasma of normal and headache rats after oral administration of Wu-Zhu-Yu decoction by a novel ultra fast liquid chromatography-tandem mass spectrometry method: application to a comparative pharmacokinetics and ethological study, J. Mass Spectrom. 48 (2013) 519–532, http://dx.doi.org/10.1002/jms.3183.
[53] C.Q. Hu, F. Li, X.W. Yang, Simultaneous determination and pharmacokinetic analysis of seven alkaloids and two flavonoids from rat plasma by HPLC-DAD after oral administration of Wuzhuyu decoction, J. Asian Nat. Prod. Res. 14 (2012) 370–381, http://dx.doi.org/10.1080/10286020.2012.656093.
[54] X.W. Yang, J. Teng, Y. Wang, W. Xu, The permeability and the efflux of alkaloids of the evodiae fructus in the caco-2 model, Phytother. Res. 23 (2009) 56–60, http://dx.doi.org/10.1002/ptr.2555.

[55] J. Zhao, X. Han, X. Zhao, C. Wang, Q. Li, X. Chen, K. Bi, A sensitive liquid chromatographic-mass spectrometric method for simultaneous determination of dehydroevodiamine and limonin from Evodia rutaecarpa in rat plasma, Anal. Bioanal. Chem. 401 (2011) 289–296, http://dx.doi.org/10.1007/s00216-011-5072-6.

[56] A. Schramm, M. Hamburger, Gram-scale purification of dehydroevodiamine from Evodia rutaecarpa fruits, and a procedure for selective removal of quaternary indoloquinazoline alkaloids from Evodia extracts, Fitoterapia 94 (2014) 127–133, http://dx.doi.org/10.1016/j.fitote.2014.02.005.